Pharmacological Research 114 (2016) 13–26

Contents lists available at ScienceDirect

Pharmacological Research

journal homepage: www.elsevier.com/locate/yphrs

Perspective

Label-free versus conventional cellular assays: Functional investigations on the human histamine H_1 receptor

S. Lieb[a,1], T. Littmann[a,1], N. Plank[a,1], J. Felixberger[a], M. Tanaka[b], T. Schäfer[c], S. Krief[d], S. Elz[a], K. Friedland[c], G. Bernhardt[a], J. Wegener[e], T. Ozawa[b], A. Buschauer[a,*]

[a] Institute of Pharmacy, University of Regensburg, D-93040 Regensburg, Germany
[b] Department of Chemistry, School of Science, University of Tokyo, Tokyo, Japan
[c] Department of Chemistry and Pharmacy, Molecular and Clinical Pharmacy, Friedrich-Alexander Universität Erlangen-Nürnberg, D-91058 Erlangen, Germany
[d] Bioprojet Biotech, 35762 Saint-Grégoire, France
[e] Institute of Analytical Chemistry, Chemo- and Biosensors, University of Regensburg, D-93040 Regensburg, Germany

ARTICLE INFO

Article history:
Received 10 June 2016
Received in revised form 11 October 2016
Accepted 11 October 2016
Available online 15 October 2016

Chemical compounds studied in this article:
Histamine dihydrochloride (PubChem CID: 5818)
Betahistine dihydrochloride (CID: 68643)
Diphenhydramine hydrochloride (PubChem CID: 8980)
Cyproheptadine hydrochloride (PubChem CID: 13770)
Maprotiline hydrochloride (PubChem CID: 71478)
Fexofenadine hydrochloride (PubChem CID: 63002)
FR900359 (PubChem CID: 14101198)
Mepyramine maleate (PubChem CID: 5284451)
[^{3}H]mepyramine (PubChem CID: 656400)
2-(3-Trifluoromethylphenyl)histamine (PubChem CID: 5310982)
Histaprodifen (PubChem CID: 10447834)
Clozapine (PubChem CID: 2818)
Levocetirizine dihydrochloride (PubChem CID: 9955977)
Mirtazapine (PubChem CID: 4205)
Gallein (PubChem CID: 73685)

Keywords:
Histamine H_1 receptor
Impedimetry
Dynamic mass redistribution
Calcium assay
beta-Arrestin recruitment
Reporter gene assay

ABSTRACT

A set of histamine H_1 receptor (H_1R) agonists and antagonists was characterized in functional assays, using dynamic mass redistribution (DMR), electric cell-substrate impedance sensing (ECIS) and various signaling pathway specific readouts (Fura-2 and aequorin calcium assays, arrestin recruitment (luciferase fragment complementation) assay, luciferase gene reporter assay). Data were gained from genetically engineered HEK293T cells and compared with reference data from GTPase assays and radioligand binding. Histamine and the other H_1R agonists gave different assay-related pEC_{50} values, however, the order of potency was maintained. In the luciferase fragment complementation assay, the H_1R preferred β-arrestin2 over β-arrestin1. The calcium and the impedimetric assay depended on G_q coupling of the H_1R, as demonstrated by complete inhibition of the histamine-induced signals in the presence of the G_q inhibitor FR900359 (UBO-QIC). Whereas partial inhibition by FR900359 was observed in DMR and the gene reporter assay, pertussis toxin substantially decreased the response in DMR, but increased the luciferase signal, reflecting the contribution of both, G_q and G_i, to signaling in these assays. For antagonists, the results from DMR were essentially compatible with those from conventional readouts, whereas the impedance-based data revealed a trend towards higher pK_b values. ECIS and calcium assays apparently only reflect G_q signaling, whereas DMR and gene reporter assays appear to integrate both, G_q and G_i mediated signaling. The results confirm the value of the label-free methods, DMR and ECIS, for the characterization of H_1R ligands. Both noninvasive techniques are complementary to each other, but cannot fully replace reductionist signaling pathway focused assays.

* Corresponding author.
E-mail address: Armin.Buschauer@ur.de (A. Buschauer).
[1] These authors contributed equally to this work.

http://dx.doi.org/10.1016/j.phrs.2016.10.010
1043-6618/

1. Introduction

The discovery of the first 'antihistamines', later designated as histamine H_1 receptor (H_1R) [1] antagonists, in 1937 and the introduction of first generation antihistaminic drugs for the treatment of allergic conditions in the 1940s represent milestones in medicinal chemistry and drug research [2,3]. The success story of this well-established class of drugs was continued by the development of second generation H_1R antagonists with low central effects and reduced affinity to off-targets (for a recent review on histamine receptors and ligands cf. [4]). The identification and preclinical characterization of the first generation H_1R antagonists was based on holistic approaches, i.e., pharmacological investigations on isolated organs and proof-of-principle studies in experimental animals, e.g., guinea-pigs. Beginning with the feasibility of radioligand binding studies more than 30 years ago, there was increasing preference for reductionist over holistic approaches in the search for ligands of G protein-coupled receptors (GPCRs). Nowadays, appropriate techniques of biochemistry and molecular biology, e.g., the cloning and expression of receptors, methods for the identification and quantification of intracellular signals as well as the resolution of three-dimensional structures of the biological targets, enable the study of GPCRs at the cellular and even the molecular level. Functional assays are mainly performed on the human orthologue of the respective protein expressed in appropriate cells. However, receptor activation may not always result in a uniform cellular response [5]. Due to the complexity of signaling networks, the selection of an individual pathway, for example, the calcium or the cyclic AMP response, even though being considered characteristic of a given receptor, may be insufficient as a readout to describe the overall cellular effect. GPCRs can activate or inhibit different effectors in a ligand-specific manner, known as "functional selectivity" or "biased signaling" [6–12]. Being aware of the limitations of the assays relying on specific readouts, holistic cellular approaches should provide a more realistic picture of the overall response to a ligand-specific receptor-mediated stimulus. Optical and impedimetric methods such as dynamic mass redistribution (DMR; resonant waveguide grating, RWG) and electric cell-substrate impedance sensing (ECIS) are based on changes of the refractive index close to the surface or the electrochemical impedance of cell-covered electrodes, respectively [6,13–21]. As label-free techniques, DMR and ECIS are of special value for investigations on orphan receptors, but may also be very useful in case of well-known GPCRs such as the H_1R [22], for example, with respect to the identification of multiple signaling pathways, i. e., responses beyond those considered in conventional assays [6,15–17,19,23–26].

The canonical signaling of the human H_1R implies mainly $G_{q/11}$ protein mediated activation of phospholipase C, resulting in increased inositol-1,4,5-trisphosphate (IP3) and 1,2-diacylglycerol (DAG) levels, the mobilization of calcium ions from intracellular stores and multiple downstream effects depending on phosphorylation processes [4,27–30]. However, the H_1R was also reported to be capable of coupling to G-proteins other than $G_{q/11}$, i. e., to $G_{i/o}$ [31–33] or G_s [34], and to induce cellular responses such as the activation of nuclear factor κB (NFκB) [35] via $G\alpha_{q/11}$ and $G\beta\gamma$. Moreover, the recruitment of β-arrestins and receptor internalization upon H_1R activation [36,37] as well as H_1R/arrestin mediated cellular signaling processes, e.g., MAPK activation [38,39] were described.

Taking into consideration the possible ligand-dependent functional selectivity, the complexity of the signaling machinery and the crosstalk within biochemical networks, the characterization of ligands in focused functional assays seems incomplete. To compare the cellular effects of H_1R ligands depending on the type of readout using genetically engineered HEK293T cells, i. e., cells of an identical genetic background, we investigated a set of agonists and antagonists (Fig. 1) by DMR and ECIS in comparison to gene reporter (luciferase) assay, calcium assays (Fura-2 and aequorin), β-arrestin recruitment and radioligand competition binding.

2. Materials & methods

2.1. Histamine receptor ligands

Histamine dihydrochloride was from Acros Organics (Geel, Belgium), betahistine dihydrochloride, diphenhydramine hydrochloride, cyproheptadine hydrochloride, maprotiline hydrochloride, fexofenadine hydrochloride and clozapine were from Sigma Aldrich (Taufkirchen, Germany), mepyramine maleate was from Tocris Bioscience (Ellisville, MO, USA), levocetirizine dihydrochloride and mirtazapine were from Biotrend (Cologne, Germany). UR-KUM530 [40], 2-phenylhistamine (Ph-his), 2-(3-bromophenyl)histamine (BrPh-his) and 2-(3-trifluoromethylphenyl)histamine (CF_3Ph-his) [41,42], histaprodifen [43] and the analogues UR-BS280, -BS354, -BS355, -BS358, -BS364 and -BS365 [44] were synthesized as reported previously. The stock solutions of agonists (10 mM) were prepared with Millipore water, except for the histaprodifen derivatives (30% DMSO). The stock solutions for antagonists (10 mM) were prepared in Millipore water, except for clozapine (stock solution in 0.1 M HCl) and fexofenadine (50% DMSO). In case that compound solutions were prepared with DMSO, the final DMSO concentration was kept below 0.5% in all assays. All stock solutions were stored at −20 °C. For label-free measurements, aliquots were thawed and diluted with Leibovitz' L-15 medium (Thermo Scientific, Darmstadt, Germany) without FCS. For Fura-2, aequorin Ca^{2+} and luciferase assay, aliquots were diluted with Millipore water.

2.2. Genetically engineered cells and culture conditions

2.2.1. HEK293T-CRE-Luc-hH$_1$R and HEK293T-CRE-Luc-hH$_1$R-hMSR1 cells

Human embryonic kidney (HEK293T) cells stably expressing the firefly luciferase under the control of the cyclic AMP response element (CRE) [45] were stably co-transfected with pcDNA3.1(+)-hH$_1$R, encoding the human H_1R, and pIRESpuro3/hMSR1, encoding the human macrophage scavenger receptor [46], and maintained as published recently (HEK293T-CRE-Luc-hH$_1$R-hMSR1 cells) [20].

2.2.2. HEK293T-CRE-Luc-hH$_1$R-mtAEQ cells

To obtain cells expressing mitochondrially tagged aequorin (HEK293T-CRE-Luc-hH$_1$R-mtAEQ cells), HEK293T-CRE-Luc-hH$_1$R cells were stably co-transfected with the pcDNA3.1/zeo-mtAEQ plasmid. The medium was removed 24 h after transfection, and the cells were transferred in a 75-cm^2 culture flask with DMEM supplemented with 10% FCS. Selection was started the next day by adding medium containing hygromycin (250 μg/mL), G418 (600 μg/mL) and zeocin (40 μg/mL) (Thermo Fisher Scientific, Rockford, IL, USA).

2.2.3. HEK293T-ARRB1-hH$_1$R and HEK293T-ARRB2-hH$_1$R cells for the hH$_1$R-β-arrestin luciferase fragment complementation assay

The fusion construct of the human H_1R (the hH$_1$R cDNA was from cDNA Resource Center, Bloomsburg, PA, USA) and the C-terminal luciferase fragment (H$_1$R-ELucC) was generated using the previously described construct SSTR2-ELucC [47] by replacing the cDNA of SSTR2 by the cDNA of the H_1R. HEK293T cells were stably transfected with the pcDNA3.1/myc-HIS (B) vector encoding a β-arrestin isoform (1 or 2) N-terminally fused with the N-terminus of a green click-beetle luciferase (ELucN-ARRB1 or ELucN-ARRB2, respectively) [47], and the pcDNA4/V5-HIS (B) vector encoding H$_1$R-ELucC (Fig. S1, Supporting information). Cells

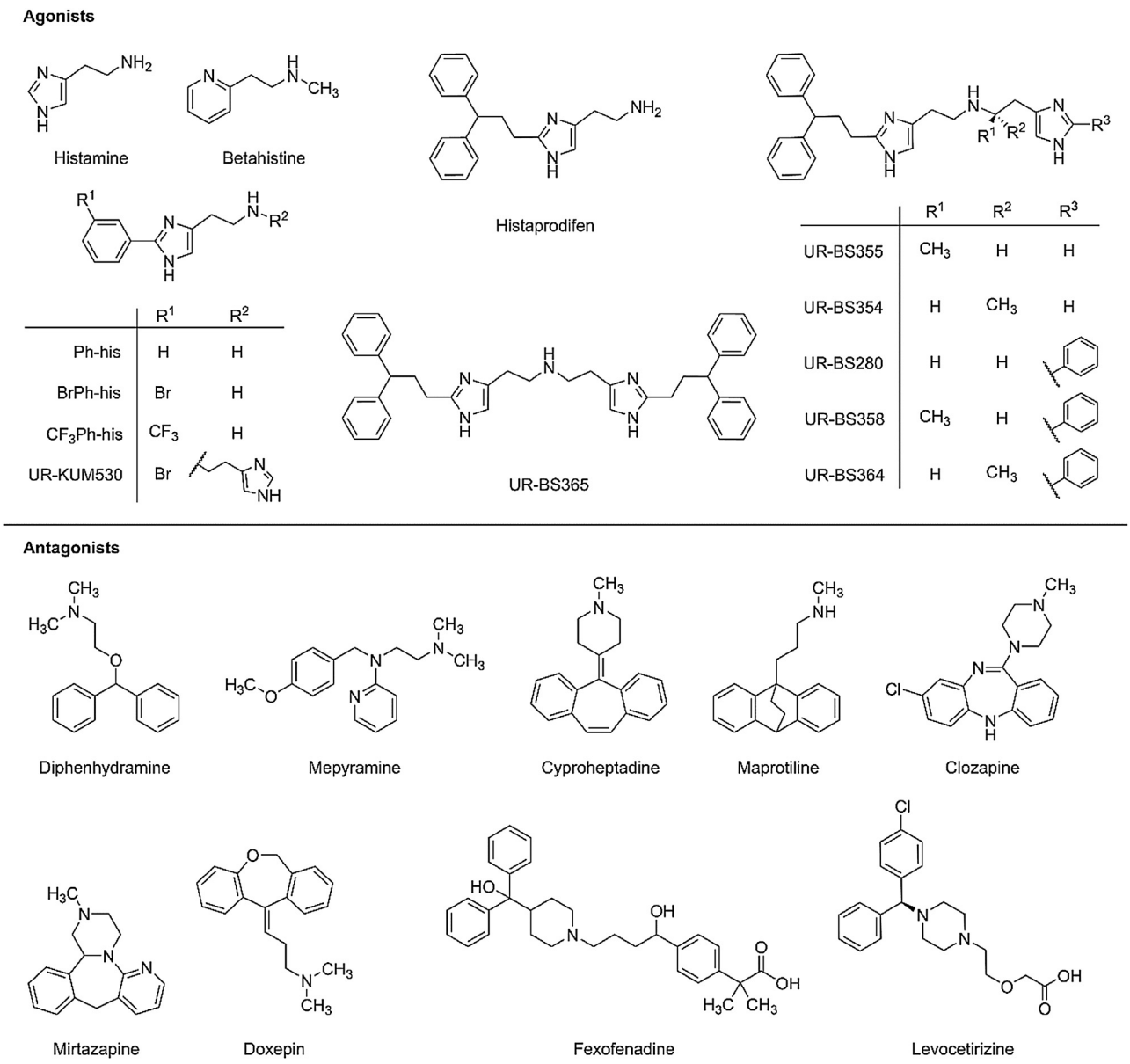

Fig. 1. Structures of compounds investigated at the human histamine H_1 receptor.

transfected with pcDNA3.1/myc-HIS (B) were cultivated in the presence of 600 μg/mL G418 for up to 3 weeks until stable growth was observed. For the cells co-transfected with the pcDNA4/V5-HIS (B) vector encoding H_1R-ELucC, 40 μg/mL zeocin was used. To determine the H_1R-ELucC expression, western blot analyses (cf. Fig. S1, Supporting information) and saturation binding studies were performed with both HEK293T-ARRB1-hH_1R cells and HEK293T-ARRB2-hH_1R cells using [^{3}H]mepyramine (cf. Fig. S2, Supporting information).

2.3. Radioligand competition binding assay

HEK293T-CRE-Luc-hH_1R cells were grown in a 75-cm^2 flask to a confluency of around 80%. The cells were detached with 5 mL of trypsin and resuspended in 5 mL Leibovitz' L-15 medium. After centrifugation, the cells were resuspended in L-15 medium. The assays were performed in the presence of 5 nM [^{3}H]mepyramine (Hartmann Analytic, Braunschweig, Germany), specific activity 20 Ci/mmol, K_d = 4.5 nM, c = 5 nM; nonspecific binding was determined in the presence of 10 μM of diphenhydramine hydrochloride (Sigma, Deisenhofen, Germany). Samples containing Leibovitzí L-15 medium, test compound (final concentration in the range from 0.1 nM to 10 μM), radioligand, and HEK293T-CRE-Luc-hH_1R cells (at a density of 1 million cells/mL), were incubated at room temperature and shaken at 250 rpm for 60 min. Filtration through glass microfiber filters (Whatman GF/C), pretreated with poly(ethylenimine) (0.3%, w/v), using a Brandel 96 sample harvester, separated unbound from cell-associated [^{3}H]mepyramine. After three washing steps with buffer (Tris, 75 mM, adjusted to pH 7.4 with HCl; $MgCl_2$, 12.5 mM; EDTA, 1 mM), filter pieces were punched and transferred into 96-well sample Plates 1450-401 (PerkinElmer, Rodgau, Germany). A volume of 200 μL of scintillation cocktail (Rotiscint Ecoplus, Roth, Karlsruhe, Germany) was added per well before incubation in the dark under shaking at 200 rpm. Radioactivity was measured with a Micro Beta2 1450 scintillation counter. Ligands were tested in at least three independent experiments each performed in triplicate.

2.4. Aequorin calcium assay

The assay was essentially performed as described previously for neuropeptide Y (NPY) Y_4 receptor ligands [48]. HEK293T-CRE-Luc-hH_1R-mtAEQ cells were detached with trypsin/EDTA and DMEM without phenol red and centrifuged at 300*g* for 10 min. The cell suspension was adjusted to a density of 10 million cells/mL in DMEM without phenol red, and coelenterazin (Biotrend) was added, so that the final concentration was 2 μM. The suspension was incubated in the dark for 2 h. The cell suspension was diluted 1:20 with loading buffer (HEPES (Serva, Heidelberg, Germany), 25 mM; NaCl, 120 mM; KCl, 5 mM; $MgCl_2$, 2 mM; $CaCl_2$, 1.5 mM; glucose 10 mM; pH was adjusted to 7.4), and the suspension was incubated in the dark under gentle stirring for additional 3 h. In the agonist mode, 18 μL of a 10-fold concentrated solution of the test compound in loading buffer were added per well of a white 96-well plate (Greiner, Frickenhausen, Germany), and luminescence was measured for 43 s with a GENios Pro microplate reader after injecting 162 μL of the cell suspension. Subsequently, 20 μL of a 1% Triton 100-X solution were injected, and light emission was recorded for additional 22 s. In the antagonist mode, 2 μL (100-fold concentrated) of the respective antagonist solution were incubated with 178 μL of the cell suspension for 15 min. Luminescence was measured after injecting 20 μL of agonist solution (10-fold concentrated) for 43 s and, subsequently, after addition of 20 μL of a 1% Triton X-100 for additional 22 s. The fractional luminescence was calculated by dividing the area of the first peak (injection of the cell suspension, respectively agonist solution) by the sum of the areas of peak 1 and peak 2 (Triton X-100 injection) using Sigma Plot 11.0 software.

2.5. Fura-2 calcium assay

The assay was essentially performed as described for NPY Y_1 receptor ligands [49]. After detachment of the cells with trypsin/EDTA, the cells were suspended in DMEM containing 5% FCS and centrifuged at 300*g* for 10 min. The medium was discarded, and the cells were resuspended in DMEM and counted. To three volumes of the cell suspension, prepared in loading buffer (HEPES (Serva), 25 mM; NaCl, 120 mM; KCl, 5 mM; $MgCl_2$, 2 mM; $CaCl_2$,1.5 mM; glucose 10 mM; pH was adjusted to 7.4), one volume of loading dispersion (1 mL of loading dispersion contained: 2% BSA (Serva); 5 μL of Pluronic (Sigma); 4 μL of Fura-2 (VWR, Ismaning, Germany)) was added, so that the final cell density was $1{\cdot}10^6$ cells per mL. The suspension was incubated in the dark for 30 min. Thereafter, the suspension was centrifuged, the cells were resuspended in loading buffer and allowed to stand in the dark for another 30 min. The cells were washed twice with loading buffer and adjusted to a final density of $1{\cdot}10^6$ cells per mL. The assay was performed either in acrylic cuvettes (VWR) using an LS50 B spectrofluorimeter (Perkin Elmer) [49] or in transparent 96-well microplates (Greiner) using a GENios Pro microplate reader [50]. Assays in the antagonist mode were always performed in cuvettes, and the cells were preincubated with the respective antagonist for 15 min.

2.6. Luciferase gene reporter assay

The assay was essentially performed as previously described for the histamine H_4 receptor [45]. One day prior to the experiments, the HEK293T-CRE-Luc-hH_1R cells were adjusted to a density of approximately $8{\cdot}10^5$ per mL in DMEM without phenol red (Sigma Aldrich) supplemented with 5% FCS. 160 μL of the cell suspension were seeded into flat bottom 96-well plates (Greiner) per well. The cells were allowed to attach overnight. In the antagonist mode, the hH_1R was stimulated by 300 nM histamine in the presence of the test compound. In the agonist mode, the H_1R was activated by 20 μL of a 10 fold concentration of the respective compound. To obtain a volume of 200 μL per well 20 μL of DMEM was added. All wells contained the same amount of DMSO or water. The medium was discarded, and 80 μL of lysis buffer (25 mM Tricine (Sigma Aldrich); Glycerol 10% (v/v) (Merck); EGTA, 2 mM (Sigma Aldrich); 1% (v/v) Triton™ X-100 (Serva); $MgSO_4 \times 7H_2O$, 5 mM (Merck); DTT, 1 mM (Sigma), the pH was adjusted to 7.8 with HCl) were added to each well. The plates were shaken at 600 rpm for 15 min. Afterwards, 40 μL of the lysate were transferred into white 96-well plates (Greiner). Luminescence was measured with a GENios Pro microplate reader (Tecan, Salzburg, Austria). Light emission was induced by injecting 80 μL of the assay buffer (25 mM Gly-Gly, (Sigma Aldrich); $MgSO_4 \times 7H_2O$, 15 mM; KH_2PO_4, 15 mM (Merck); EGTA, 4 mM; ATP disodium salt, 2 mM (Sigma Aldrich); DTT, 2 mM; D-luciferin potassium salt, 0.2 mg/mL (Synchem, Felsberg, Germany); pH was adjusted to 7.8 with HCl). Luminescence [51] was measured for 10 s. To determine the effect of pertussis toxin (PTX) cells were seeded in medium containing 100 ng/mL PTX. For experiments in the presence of FR900359 (UBO-QIC; Institute of Pharmaceutical Biology, University of Bonn, Germany) (1 μM and 10 μM) or gallein (Santa Cruz Biotechnology, Heidelberg, Germany) (20 μM, stock solution: 10 mM in DMSO), cells were pre-incubated with the $G\alpha_q$ inhibitor or the $G\beta\gamma$ inhibitor for 2 h. By analogy experiments were performed after pre-incubation of the cells in the presence of 100 μM of the protein kinase A inhibitor Rp-cAMP-S or Rp-8-Br-cAMP-S (Santa Cruz Biotechnology; stock solutions: 10 mM in water) for 1 h.

2.7. β-Arrestin recruitment assay

One day before the experiment, HEK293T-ARRB1-H_1R and HEK293T-ARRB2-H_1R cells were trypsinized (0.05% trypsin, 0.02% EDTA in PBS) and centrifuged (400*g*, 5 min). The cells were resuspended in DMEM without phenol red (Sigma, Steinheim, Germany) supplemented with 5% FCS, and 90 μL of the cell suspension were seeded in white, TC-treated, flat bottom 96-well microtiter plates (VWR, Ismaning, Germany) at a density of approximately 100,000 cells/well. The cells were cultivated at 37 °C overnight in a water-saturated atmosphere containing 5% CO_2. Shortly before the experiment, the cells were removed from the incubator and allowed to equilibrate to room temperature, and 10 μL of agonist solution were added per well. The plates were shaken at 25 °C for 60 min. In the antagonist mode, prior to addition of the agonist, cells were incubated with the respective antagonist for 15 min. At the end of the incubation period, 50 μL of medium were replaced by 50 μL of Bright-Glo luciferase assay reagent (Promega, Mannheim, Germany). The plates were vigorously shaken (800 rpm) for 5 min. Bioluminescence was recorded for 1 s per well using the GENios Pro microplate reader (Tecan, Salzburg, Austria).

2.8. Impedimetric assay

For the investigation of H_1R agonists on HEK293T-CRE-Luc-hH_1R-hMSR1 cells, the assay was performed as recently described for histamine [20] using an ECIS-Z device for 96-well electrode arrays (type 96W1E+) from Applied BioPhysics (Troy, NY, USA). A volume of 300 μL of cell suspension, prepared in DMEM containing 10% FCS from close-to-confluent cell layers by standard trypsinization techniques, was dispensed at a density of $9{\cdot}10^4$ cells per well. The cells were allowed to attach in a CO_2 incubator at 37 °C for 24 h. About 1 h before the assay the culture medium was replaced by 150 μL of serum-free L-15 medium. Data were recorded with the ECIS device inside an incubator (Galaxy 48S, New Brunswick, USA) in a humidified atmosphere (without additional CO_2) at 37 °C at an AC frequency of 4 kHz for 1 h until the baseline was constant

(equilibration), and for another 40 min after addition of the agonist at various concentrations. For data handling cf. [20].

Time course data is presented as the change in impedance magnitude $\Delta|Z|(t)$ relative to the last data point before test compounds were added into the wells at time zero ($\Delta|Z|(t) = |Z|(t) - |Z|(0)$). The time courses for all test compounds were subsequently corrected for the corresponding values of untreated controls (buffer only). Concentration-response curves were constructed from the area under the curve (AUC) calculated from corrrected time coursesc of individual response profiles from 0 to 40 min for each compound concentration.

For the determination of H_1R antagonist activities, after equilibration for 1 h, 150 μL a solution of the respective antagonist was added to the cells for an incubation period of about 20 min. Subsequently 150 μL of the antagonist containing solution was replaced by the same volume of L-15 medium containing the antagonist at the same concentration and 60 nM of histamine to obtain a final agonist concentration of 30 nM, which is known to elicit 80% of the maximal response in the absence of an antagonist.

The effect of pertussis toxin (PTX) was determined in the agonist mode using cells pretreated with 1, 10 or 100 ng/mL PTX in DMEM supplemented with 10% FCS for about 20 h. About 1 h before the assay the culture medium was replaced by 150 μL of serum-free L-15 medium and the assay was performed as described above. To investigate the effect of FR900359, by analogy with the antagonist mode, cells were preincubated in the presence of the $G\alpha_q$ inhibitor at final concentrations of 0.1, 1 or 10 μM for 20 min.

2.9. Dynamic mass redistribution assay

The assay was performed in the agonist mode as previously described for histamine on HEK293T-CRE-Luc-hH_1R-hMSR1 cells [20] using an EnSpire (PerkinElmer, Waltham, USA) multimode reader. A volume of 40 μL of cell suspension, prepared from close-to-confluent cell layers by standard trypsinization, in DMEM containing 10% FCS was dispensed at a densitiy of $2{\cdot}10^4$ cells per well into uncoated 384-well EnSpire microplates. Incubation in a humidified atmosphere containing 5% CO_2 at 37 °C for 24 h provided cell layers of approximately 90 % confluency. The cells were washed four times with serum-free L-15 medium and allowed to equilibrate in a volume of 30 μL of the same medium per well in the multimode reader at 37 °C for about 1 h. After recording the baseline, the agonist of interest, dissolved in L-15 medium (10 μL) was added, the cellular response was recorded for 40 min and data analysis was performed as described [20].

Time course data is presented as the shift of resonance wavelength $\Delta\lambda\,(t)$ relative to the last data point before test compounds were added into the wells at time zero ($\Delta\lambda\,(t) = \lambda\,(t) - \lambda\,(0)$). The time courses for all test compounds were subsequently corrected for the corresponding values of untreated controls (buffer only). Concentration-response curves were constructed from the area under the curve (AUC) calculated from corrrected time courses of individual response profiles from 0 to 40 min for each compound concentration.

In the antagonist mode, after equilibration in 30 μL of medium per well for 1 h, a solution of the respective antagonist in 10 μL of serum-free L15 medium was added, and the incubation was continued for 20 min. Subsequently, another 10 μL of antagonist at the same concentration containing additionally 500 nM of histamine to obtain a final agonist concentration of 100 nM, which is known to elicit 80% of the maximal response in the absence of an antagonist.

The effect of pertussis toxin (PTX) was determined in the agonist mode using cells pretreated with 1, 10 or 100 ng/mL PTX in DMEM supplemented with 10% FCS for about 20 h. The cells were washed four times with serum-free L-15 medium and the assay was performed as described above. Experiments in the presence of FR900359 were performed according to the antagonist mode with the exception that instead of antagonist the $G\alpha_q$ inhibitor was added at final concentrations of 0.1, 1 or 10 μM.

2.10. Data processing

The data were analyzed with GraphPad Prism 5.01 (GraphPad Software, San Diego, USA) and fitted to four-parameter sigmoidal concentration-response curves providing EC_{50} values of agonists and IC_{50} values of antagonists. For antagonists, pK_b values were calculated from IC_{50} values according to the Cheng-Prusoff equation [52]. Statistical analyses of ΔpEC_{50} and E_{max} values were performed according to a one-way ANOVA using Bonferroni's post-hoc test. In case of less than three types of assays (histaprodifen), an unpaired two-tailed *t*-test was performed. In case of the antagonists, the pK_b values from each assay were compared to the pK_i values obtained from competition binding studies by a two-way ANOVA with Bonferroni's post-hoc test.

3. Results & discussion

The functional experiments were performed on HEK293T transfectants with roughly comparable levels of hH_1R expression as proven by saturation binding experiments with [^{3}H]mepyramine (cf. Supplementary information, Fig. S2).

3.1. Functional characterization of agonists on H_1R expressing HEK293T transfectants

3.1.1. Agonist activity of histamine with emphasis on data from label-free methods

Changes of the resonance wavelength of cell-covered optical waveguides (resonance waveguide = RWG), recorded in DMR, or of the impedance of cell-covered electrodes, measured in ECIS, reflect alterations in cell shape and structure [25,53–55]. As demonstrated in a recent study, cell adhesion to the surface is a critical issue in such label-free assays [20]. The DMR assay reports on changes in mass distribution *inside* the cell close to the growth surface or *outside* the cell in the narrow cleft between cell and substrate. Mass redistribution and cell shape changes may be connected in the way that mass redistribution induces cell shape changes or *vice versa*, although difficult to prove or disprove. It is reasonable to assume that the signal is dominated by dynamic processes that occur *within* the actin cortex or by remodeling *of* the actin cortex at the membrane in the vicinity of the growth support [53–55]. In this context, it is noteworthy that the thickness of the actin cortex is 100 to 1000 nm depending on cell-type. DMR is only sensitive within 200 to 300 nm from the substrate surface. The actin cortex is not necessarily the exclusive origin of the DMR signal, since relocation of other, even extracellular (macro)molecules that are not linked to the actin cortex or the membrane, can cause similar responses. This is different from ECIS, which is insensitive to mass redistribution, but reflects changes in the ionic current pathways around or across the dielectric lipid bilayer, primarily associated with alterations in cell morphology. Due to the intimate molecular contact between the lipid bilayer of the plasma membrane and the adjacent actin cortex, changes in the position of the membrane are invariably associated with a concomitant relocation of the actin cortex so that both readout techniques often, but not always, report on similar phenomena. Thus, some cellular responses leading to mass redistribution, but not to changes in the position of the membrane relative to the growth support, become visible in DMR but not in ECIS, and the information gained from both readouts is not identical but complementary.

Therefore, we performed both, DMR and ECIS, with HEK293T-CRE-Luc cells engineered to co-express the human histamine

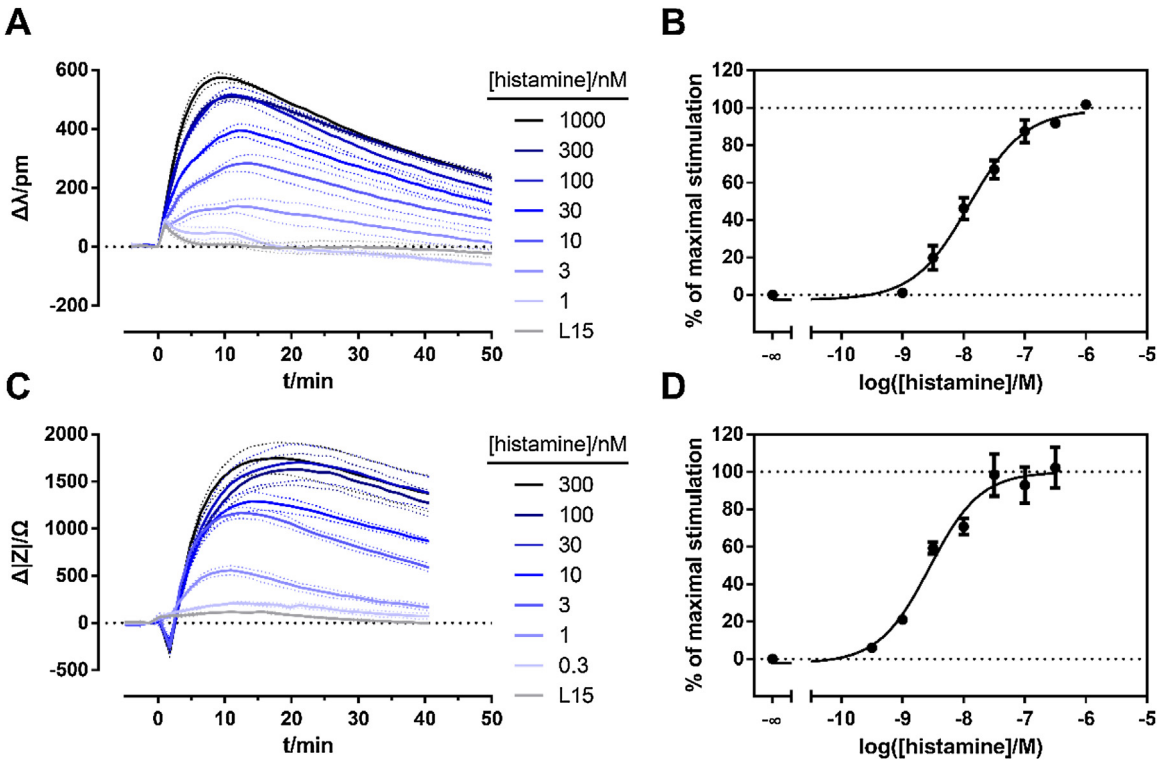

Fig. 2. Histamine induced response of HEK293T-CRE-Luc-hH$_1$R-hMSR1 cells monitored by DMR (A, B) and ECIS (C, D). Typical time courses (triplicates) of the change of the resonance wavelength (A) and the change in impedance Δ|Z| recorded at 4 kHz (C). Concentration-response curves (B, D) were derived from the corresponding area-under-the-curve (AUC) of baseline-corrected data integrated from 0 to 40 min.

H_1 receptor and the human macrophage scavenger receptor 1 (hMSR1) [56], to improve adhesion as described previously [20]. Both label-free assays were performed under similar conditions, e.g., with respect to temperature, cell-culture medium and equilibration time. Typical time courses and the resulting concentration-response curves are shown in Fig. 2 for histamine. The transient dip of the impedimetric signal observed immediately after addition of the agonist is considered characteristic of G_q coupling [30], allowing for a discrimination from G_i coupling.

The DMR signal at the highest histamine concentration peaks after an exposure time of approximately 10 min, whereas the ECIS signal is retarded and peaks between 15 and 20 min after addition of histamine. This indicates that agonist-induced mass redistribution precedes cell shape changes, at least at higher histamine concentrations.

The construction of concentration-response curves revealed pEC_{50} values of 7.49 ± 0.08 and 7.92 ± 0.16 for histamine in the DMR assay and ECIS, respectively. Comparing the data summarized in Table 1 and visualized in Figs. 2 and 3, the apparent potencies of histamine differ by up to a factor of approximately 10, depending on the type of assay. The highest pEC_{50} values of histamine was determined in the impedance-based (7.92) and the β-arrestin2 recruitment assay (7.74), whereas the luciferase gene reporter and the Fura-2 calcium assay yielded the lowest potency ($pEC_{50} = 6.87$).

3.1.2. H_1R agonism of histamine in various assays: Investigation of G protein coupling

To investigate the contribution of $G_{i/o}$ and $G_{q/11}$ proteins, we constructed concentration-response curves of histamine in the presence of pertussis toxin (PTX) [31] or the cyclic depsipeptide FR900359 [57,58], respectively (Fig. 3; for concentration-response curves of UR-KUM530 alone and in the presence of G-protein inhibitors: cf. Supporting information).

As becomes obvious from Fig. 3, the histamine response was reduced to a different extent by the $G_{q/11}$ inhibitor FR900359, depending on the assay. The impedance-based readout as well as the aequorin calcium assay revealed a complete lack of response to histamine in the presence of FR900359 at concentrations of 0.1 μM (not shown) and 1 μM, respectively. By contrast, the DMR signal was reduced by approximately 80% and the luciferase activity (gene reporter assay) was lowered by about 50% in the presence of FR900359 at a concentration of 1 μM, and the maximal responses could not be further suppressed by FR900359 at a concentration of 10 μM (not shown). Whereas the blockade of the calcium signal was expected due to $G_{q/11}$ inhibition, the differential effects of FR900359 in the two holistic assays (ECIS and DMR) and on the luciferase activity suggested additional signaling pathways to contribute to the respective readouts (DMR and gene reporter assay) upon H_1R stimulation.

In the presence of pertussis toxin at concentrations from 1 to 100 ng/mL, the impedance of the histamine-stimulated cells signal remained almost unaffected (Fig. 3), i. e., there was no indication of a contribution of G_i to the impedimetric response. This observation was in agreement with the complete blockade by the G_q inhibitor FR900359. On the contrary, PTX decreased the response in DMR in a concentration-dependent manner resulting in complete blockade at a concentration of 100 ng/mL. Although the DMR response was also strongly suppressed by FR900359, the results demonstrate that G_i is involved, too. This phenomenon is reminiscent of promiscuous GPCRs capable of coupling to G_q and G_i, as reported for the free fatty acid receptor FFA1 [58], and depending on the cell type, the H_1R was described to couple to G_q and/or G_i [31,34,59]. This is supported by the effect of PTX on the histamine-induced luciferase activity in the gene reporter assay (Fig. 3). Inhibition of G_i by PTX (100 ng/mL) resulted in an increase in bioluminescence by approximately 75%. The HEK293T-CRE-Luc-hH1R cells were engi-

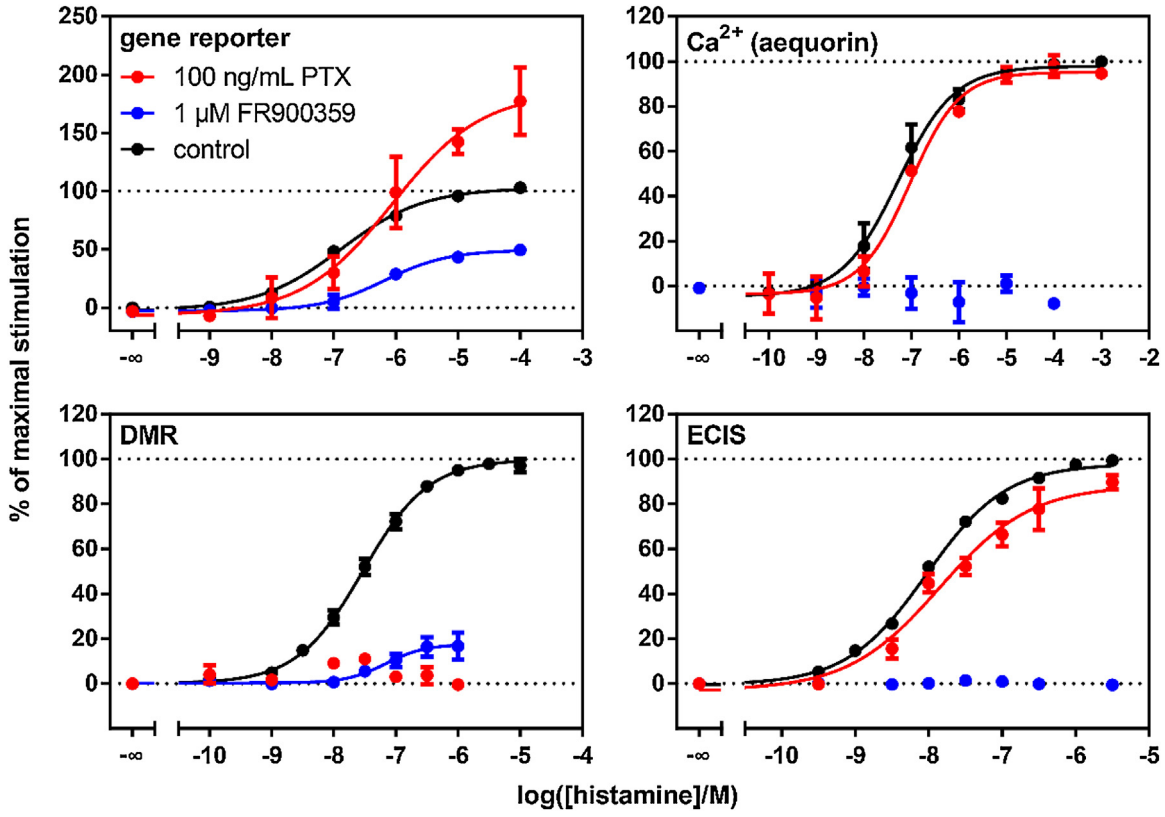

Fig. 3. Effect of the G_q-inhibitor FR900359 and G_i-inhibitor pertussis toxin (PTX) on the histamine-induced response in DMR, ECIS, gene reporter and Ca^{2+} (aequorin) assays. Experiments were performed using HEK293T cells expressing hH_1R and additional constructs: DMR and ECIS: HEK293T-CRE-Luc-hH_1R-hMSR1 cells; luciferase gene reporter: HEK293T-CRE-Luc-hH1R cells; aequorin calcium assay: HEK293T-CRE-Luc-hH_1R-mtAEQ cells. Cells were incubated with FR900359 for 2 h (gene reporter and aequorin assay) or 20 min (DMR and ECIS), and with PTX for 16 h (gene reporter and aequorin assay), or 20 h (DMR and ECIS). Data were normalized to a solvent control and the maximal activation of each system (100%) by the endogenous ligand histamine, respectively. Data represent means ± SEM from at least two independent experiments performed in triplicate. Note: Control experiments (gene reporter assay) performed with the three HEK293T cell variants revealed that the histamine induced luciferase activity was comparable (signal-to-noise ratio approximately 25) for HEK293T-CRE-Luc-hH_1R and HEK293T-CRE-Luc-hH_1R-hMSR1 cells, whereas the signal-to-noise ratio was by a factor of approximately 3 lower in case of HEK293T-CRE-Luc-hH_1R-mtAEQ cells (cf. Supporting information, Fig. S3). The fact that PTX is fully effective to inhibit G_i-mediated cellular response at a concentration of 100 ng/mL becomes obvious from control experiments performed with HEK293T-CRE-Luc-hH4R cells [45] shown in the Supporting information (Fig. S4).

neered to detect the cyclic AMP dependent expression of luciferase. However, in case of H_1R stimulation, the increase in luciferase activity is elicited by G_q-coupling resulting in a mobilization of Ca^{2+} from the endoplasmic reticulum (cf. Supporting information, Fig. S5), and, for example, in subsequent calcium-calmodulin dependent phosphorylation of the CRE binding protein (CREB) [60–62]. The increase in bioluminescence in the presence of PTX confirms the contribution of G_i as an inhibitory component in this assay. Calcium-calmodulin can also activate adenylyl cyclases [63] and a subsequent increase in the luciferase activity can result from protein kinase A (PKA) dependent phosphorylation of CREB. Therefore, we constructed concentrations-response curves of histamine alone and in the presence of the PKAI and PKAII inhibitors Rp-cAMP-S and Rp-8-Br-cAMP-S [64]. At high concentrations (100 µM), both PKA inhibitors reduced the luciferase signal by about 50%, and in combination with FR900359 (1 µM) the response was almost completely suppressed (data not shown). Therefore, unspecific effects of the moderately active inhibitors and contributions from additional signaling pathways cannot be ruled out.

Generally, the Gβγ dimer is also capable of interacting with effector proteins. For instance, Gβγ can interfere with the cAMP pathway [65–67] and can trigger an intracellular increase in intracellular Ca^{2+} by interacting with phospholipase C and Ca^{2+} channels [68]. Very recently, regardless of its selectivity for $G\alpha_q$ over $G\alpha_i$ and $G\alpha_s$ [58], FR900359 was reported to inhibit Gβγ-mediated signaling, too [69]. In this context, we investigated the influence of gallein, which is supposed to be a reversible inhibitor of Gβγ with a K_d value of 422 nM [70,71]. In the presence of gallein at a concentration of 20 µM, the concentration-response curve of histamine in the luciferase gene reporter assay on HEK293T-CRE-Luc-hH_1R cells remained unaffected (data not shown), suggesting that the Gβγ dimer is not involved (for control experiments on the inhibition of a Gβγ mediated response, the dopamine D_2 receptor stimulated Na^+ influx [72] in HT22 cells, by gallein: cf. Supporting information, Fig. S6).

With respect to the two label-free approaches, it is noteworthy that ECIS reads primarily G_q-mediated changes of the cell shape upon histamine stimulation, as FR900359 completely inhibits the cellular response. Consistent with the inhibition of the calcium signal in the aequorin assay, experiments with a calcium ionophore using U-373 MG cells, constitutively expressing the H_1R, revealed that an increase in intracellular Ca^{2+} alone was sufficient to produce ECIS traces very similar to those upon histamine stimulation (data not shown). The dependence of the ECIS signal on the increase in $[Ca^{2+}]_i$ is plausible due to (i) the predominant influence of the actin cortex on membrane topography/cell shape and (ii) the fact that $[Ca^{2+}]_i$ is a well-known modulator of cortical actin (in concert with myosin). Other signaling pathways that are potentially triggered by histamine are not mirrored in the signal, when they are not linked to cortical actin or reorientation of the membrane. In DMR

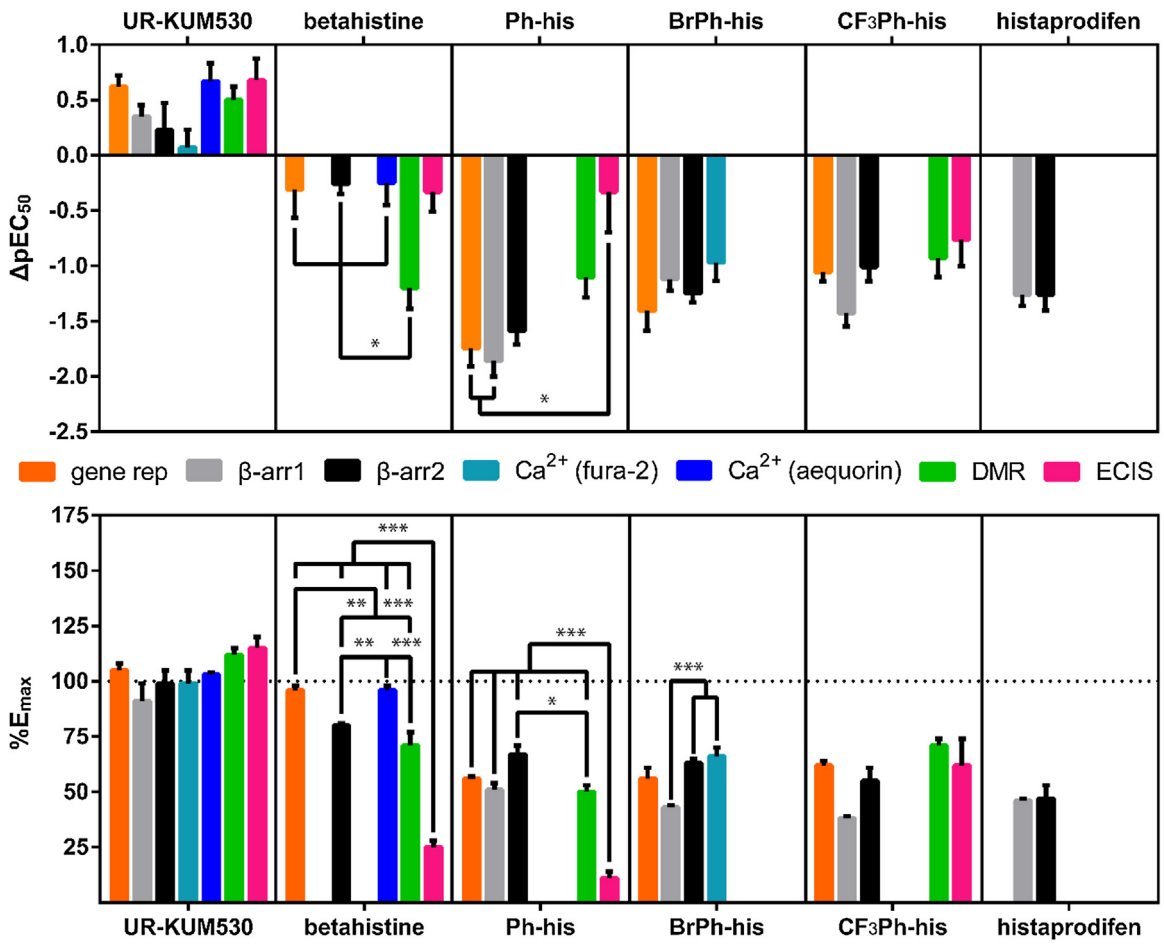

Fig. 4. Relative H_1R agonist potencies, expressed as ΔpEC_{50} (±SEM) and intrinsic activities (E_{max} ± SEM) referred to histamine in the respective assay. Histamine: $\Delta pEC_{50} = 0$, $E_{max} = 1.0$. Calculated from the data given in Table 1. ΔpEC_{50} values were calculated for each ligand by subtracting the pEC_{50} value in the respective assay from the pEC_{50} value of histamine in the same assay considering error propagation. For further statistical analyses, the number of independent experiments (*N*) with the particular ligand were considered. In order to obtain information on statistical differences between ΔpEC_{50} and E_{max} values of the different ligands in the same assay, one-way ANOVA analyses (Bonferroni's post-hoc test) were performed for every data set, except for histaprodifen (unpaired two-tailed *t*-test). Data from different assays are not significantly different from each other ($P > 0.05$) unless otherwise indicated by asterisks (*: $P < 0.05$; **: $P < 0.01$; ***: $P < 0.001$). Note, for the sake of clarity concerning E_{max} values of betahistine: gene rep. vs. β-arr2: $P < 0.01$, gene rep. vs. DMR: $P < 0.001$; aequorin vs. β-arr2: $P < 0.01$, aequorin vs. DMR: $P < 0.001$.

assays, the G_q inhibitor FR900359 could not entirely block the agonist induced response, whereas the G_i inhibitor PTX almost entirely reduced the signal. Thus, DMR records a response integrating both G_q and G_i-mediated signaling.

3.1.3. Cellular responses to different H_1R agonists in various assays

To investigate, whether activation of the H_1R by ligands other than histamine yields different assay-related relative potencies (ΔpEC_{50} values, referred to histamine in the respective assay), we selected the agonists shown in Fig. 1 for functional studies. All agonists included in this study preferentially induced the recruitment of β-arrestin2 over the β-arrestin1 isoform as generally observed for class A GPCRs [75]. Unfortunately, it turned out that not all of these compounds are compatible with the different types of assay. In particular, the histaprodifen analogues [73], designated UR-BS compounds in the present study, caused cytotoxic effects at concentrations >1 μM (for cytotoxicity of selected compounds cf., Supporting information, Fig. S7), most probably due their amphiphilic nature. Although the β-arrestin recruitment assays revealed partial agonism in the expected concentration range (cf. Table S1 and Fig. S8, Supporting information), attempts to characterize such compounds in ECIS and in the Fura-2 calcium assay using U373 MG cells [20] as well as in the luciferase gene reporter assays failed (data not shown). In contrast to the UR-BS compounds, the phenylhistamine derivative UR-KUM530 [40] proved to be non-toxic up to a concentration of 100 μM (cf. Fig. S7A, Supporting information), allowing for the determination of pEC_{50} values in both, the label-free and the conventional assays. As becomes obvious from Table 1, Figs. 4 and 5, UR-KUM530 was more potent than histamine in all assays and appeared to be a super-agonist in both, the impedimetric and the DMR assay. However, the E_{max} values of UR-KUM530 in ECIS and DMR were statistically not different from the maximal responses in the other assay. Interestingly, the concentration-response curve from ECIS is exceptionally steep, resulting in about 30-fold higher potency than in the Fura2 assay. The time course of the impedimetric signal was similar to that of histamine with regard to the initial dip and the subsequent rise, suggesting G_q coupling for this compound, too (data not shown). By contrast, the investigation of betahistine revealed completely different concentration-response curves (Fig. 5): full agonism in the aequorin calcium and the luciferase gene reporter assay (E_{max}: 0.96), but only partial agonism in β-arrestin2 recruitment (E_{max}: 0.80), DMR (E_{max}: 0.71) and, in particular, in the impedimetric assay (E_{max}: 0.25). The extremely low intrinsic activity observed in the ECIS assay cannot be explained. Regardless of the

Table 1
hH_1R agonism determined in different functional assays using genetically engineered HEK293T cells.[a,b] For comparison published functional data from [^{32}P]GTPase assays[c] are included.

	gene reporter (luciferase)		β-arrestin1 recruitment		β-arrestin2 recruitment		Ca^{2+} (Fura-2 AM)		Ca^{2+} (aequorin)		DMR		ECIS		GTPase [40,73,74]	
	pEC_{50}	E_{max}	pEC_{50}	E_{max}	pEC_{50}	E_{max}	pEC_{50}	E_{max}	pEC_{50}	E_{max}	pEC_{50}	E_{max}	pEC_{50}	E_{max}	pEC_{50}	E_{max}
histamine	6.87 ± 0.06	1.00	7.11 ± 0.1	1.00	7.74 ± 0.08	1.00	6.87 ± 0.06	1.00	6.94 ± 0.15	1.00	7.49 ± 0.08	1.00	7.92 ± 0.16	1.00	6.92 [73]	1.00
UR-KUM530	7.49± 0.08	1.05 ± 0.03	7.46 ± 0.03	0.91 ± 0.08	7.97 ± 0.23	0.99 ± 0.06	6.94 ± 0.02	0.99	7.61 ± 0.06	1.03 ± 0.01	7.99 ± 0.09	1.12 ± 0.03	8.60 ± 0.11	1.15 ± 0.05	7.75 [40]	0.94
betahistine	6.56 ± 0.25	0.96 ± 0.02			7.48 ± 0.04	0.80 ± 0.01	n.d.	–	6.69 ± 0.13	0.96 ± 0.02	6.29 ± 0.17	0.71 ± 0.06	7.59 ± 0.08	0.25 ± 0.03	5.85 [74]	0.86
Ph-his	5.12 ± 0.15	0.56 ± 0.01	5.25 ± 0.10	0.51 ± 0.03	6.15 ± 0.09	0.67 ± 0.04	n.d.	–	n.d.		6.39 ± 0.17	0.50 ± 0.03	7.59 ± 0.33	0.11 ± 0.03	6.14 [40]	0.72
BrPh-his	5.46 ± 0.17	0.56 ± 0.05	5.99 ± 0.03	0.43 ± 0.01	6.49 ± 0.01	0.63 ± 0.02	5.90 ± 0.07	0.66	n.d.		n.d.		n.d.		6.75 [40]	0.62
CF_3Ph-his	5.81 ± 0.06	0.62 ± 0.02	5.68 ± 0.06	0.38 ± 0.01	6.73 ± 0.10	0.55 ± 0.06	n.d.	–	n.d.		6.56 ± 0.15	0.71 ± 0.03	7.16 ± 0.18	0.62 ± 0.12	6.71 [40]	0.61
histaprodifen			5.85 ± 0.02	0.46 ± 0.01	6.48 ± 0.12	0.47 ± 0.06	n.d.	–	n.d.		n.d.		n.d.		6.95 [73]	0.62

[a] Experiments were performed using HEK293T cells expressing hH_1R and additional constructs: luciferase gene reporter: HEK293T-CRE-Luc-hH1R cells; β-arrestin recruitment assay: HEK293T-ARRB1-H_1R and HEK293T-ARRB2-H_1R cell; Fura-2 calcium assay: HEK293T hH_1R CRE-Luc cells; aequorin calcium assay: HEK293T-CRE-Luc-hH_1R-mtAEQ cells; DMR and impedimetry (ECIS): HEK293T-CRE-Luc-hH_1R-hMSR1 cells.

[b] Data represent mean values ± SEM from at least three independent experiments performed in triplicate, except for UR-KUM530 and BrPh-his in the Fura-2 AM Ca^{2+}-assay and BrPh-his and CF_3Ph-his in the gene reporter assay, which were analyzed in two independent experiments performed in triplicate; n.d., not determined.

[c] Determined on membranes of hH_1R expressing Sf9 cells. For hH_1R binding data determined on membranes of Sf9 cells cf. [40,73].

Table 2
pK_b-values for hH_1R antagonists determined in different functional assays and pK_i-values determined in radioligand competition binding studies.

H_1R antagonist'	gene reporter (luciferase)	β-arrestin2 recruitment[a]	Ca^{2+} (Fura-2 AM)	Ca^{2+} (aequorin)	DMR[b]	ECIS[c]	GTPase[d]	competition binding
diphenhydramine	7.66 ± 0.24	7.96 ± 0.04**	7.43 ± 0.08	7.62 ± 0.05	7.55 ± 0.05	7.59 ± 0.10	7.81 [74]	7.40 ± 0.03
mepyramine	8.13 ± 0.10	8.08 ± 0.09	8.85 ± 0.01	8.39 ± 0.12	8.43 ± 0.11	8.70 ± 0.14	8.25 [74]	8.39 ± 0.04
cyproheptadine	8.55 ± 0.11	8.60 ± 0.06	8.60 ± 0.03	7.99 ± 0.13	8.01 ± 0.14	10.15 ± 0.28***	8.72 [74]	8.63 ± 0.05
maprotiline	8.47 ± 0.12	8.38 ± 0.03	8.58 ± 0.08	8.00 ± 0.05	8.19 ± 0.13	8.84 ± 0.53	8.54 [78]	8.50 ± 0.05
fexofenadine	7.47 ± 0.03***	6.95 ± 0.03	6.85 ± 0.09	6.29 ± 0.03	7.01 ± 0.03	8.23 ± 0.30***	6.65 [74]	6.70 ± 0.06

Functional studies were performed using genetically engineered HEK293T cells (cf. Table 1, footnote) and histamine as agonist. Binding data were determined on HEK293T-CRE-Luc-hH_1R cells. pK_b-values determined by each particular functional assay are not significantly different ($P > 0.05$) from pK_i values determined by competition binding unless otherwise indicated by asterisks (two-way ANOVA with Bonferroni post hoc test. *: $P < 0.05$; **: $P < 0.01$; ***: $P < 0.001$). Data represent means ± SEM from at least three independent experiments performed in triplicate. Functional and binding data of additional H_1R antagonists investigated in the respective assay, pK_b values: [a]levocetirizine, 7.16 ± 0.07; mirtazapine, 8.71 ± 0.07, clozapine, 7.64 ± 0.05. [b]Mirtazapine, 8.46 ± 0.10; doxepine, 9.35 ± 0.19; clozapine, 8.21 ± 0.22. [c]Levocetirizine, 8.72 ± 0.14; doxepine, 9.11 ± 0.28; clozapine, 9.60 ± 0.08. [d]Mirtazapine 8.59 [78]; doxepine, 8.90 [78]; clozapine, 8.36 [78].

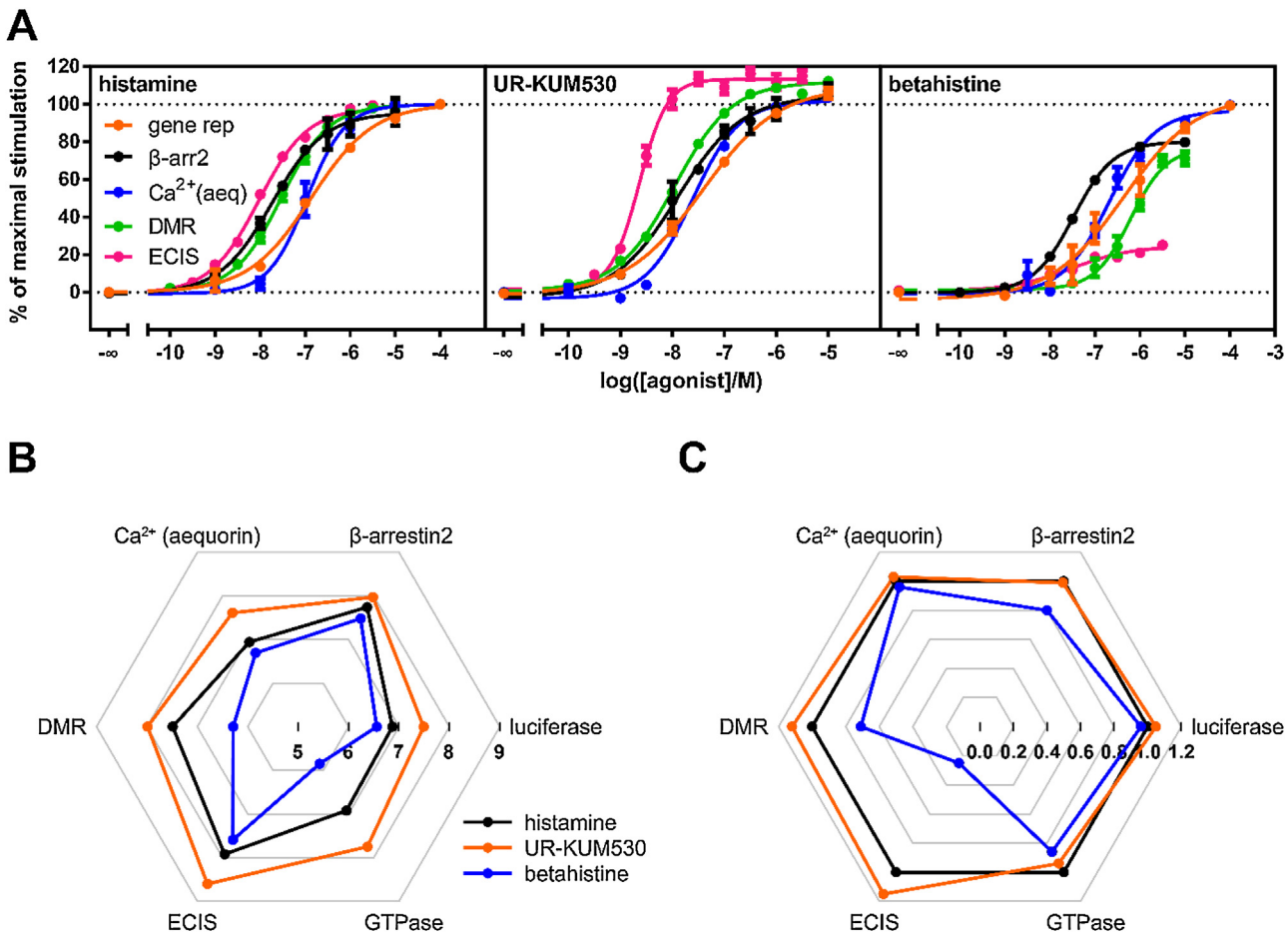

Fig. 5. Assay-dependent concentration-response curves of histamine, UR-KUM530 and betahistine (A). Spider plots representing pEC_{50} values (B) and efficacies (C). Experiments were performed using HEK293T cells expressing the hH_1R and additional constructs: gene rep (luciferase gene reporter assay): HEK293T-CRE-Luc-hH_1R cells; βarr2 (β-arrestin2 recruitment assay): HEK293T-ARRB2-hH_1R cells; Ca^{2+}(aeq) (aequorin calcium assays): HEK293T-CRE-Luc-hH_1R-mtAEQ cells; DMR and ECIS: HEK293T-CRE-Luc-hH_1R-hMSR1 cells. Data were normalized to a solvent control and the maximal response to the endogenous ligand histamine in the respective assay. Data represent means ± SEM from at least three independent experiments performed in triplicate.

weak increase in Δ|Z|, a transient dip of the signal was observed as for histamine and UR-KUM530 (data not shown). The relative agonist potency was comparable in all assays except for DMR, where betahistine was by a factor of ten less potent (Fig. 4).

In cells of one and the same genetic background (HEK293T-CRE-Luc-hH_1R for calcium, luciferase gene reporter, DMR and impedance-based functional assays) our data illustrate that the measured potencies and maximal responses vary depending on both, the readout and the chemical structure of the agonist. This becomes obvious from concentration-response curves and, in particular, from the spider plot in Fig. 5. The potencies of histamine and UR-KUM530 in the luciferase gene reporter assay were similar to those obtained in assays exploiting the GTPase activity as a proximal readout (Table 1). The efficacy of UR-KUM530 was the same as that of histamine except for both label-free assays, which gave a slightly higher maximal response (Fig. 4). This might be interpreted as "superagonism" [76] related to different binding modes of histamine and UR-KUM530 [40], resulting in a differential activation of signaling pathways. However, the inhibition of the cellular signal by FR900359 and PTX upon stimulation with UR-KUM530 was qualitatively the same as in case of histamine (cf. Fig. S9, Supporting information, vs. Fig. 3). There was no indication of a differential activation of signaling pathways, when comparing both H_1R agonists. In principle, potencies and intrinsic activities depend on receptor density [77]. However, the levels of H_1R expression of the studied transfectants was comparable (cf. Supporting information, Fig. S2).

The response to UR-KUM530 was completely inhibited by diphenhydramine (100 μM) or mepyramine (10 μM) in both assays, DMR and ECIS, confirming that the effects were H_1R mediated (data not shown). The pK_b values determined from the corresponding inhibition curves were 7.68 ± 0.24 and 8.48 ± 0.44 in ECIS and 7.07 ± 0.11 and 8.64 ± 0.32 in DMR for diphenhydramine and mepyramine, respectively, which is comparable to the respective values determined versus histamine as agonist (Table 2).

The assay-dependent differences regarding relative potencies (ΔpEC_{50}) and E_{max} values (Fig. 4) observed for all agonists under study are difficult to explain, as not all assays can be performed under identical conditions. However, the order of potency of agonists was roughly the same between the noninvasive and the canonical assays.

3.2. Functional characterization of H_1 receptor antagonists

Functional studies were performed with structurally diverse H_1R antagonists representing different generations of antihistaminics (Fig. 1). The data of compounds analyzed in both, the label-free and the conventional assays, are summarized in Table 2, and concentration-response curves are depicted in Fig. 6. For comparison, data of those compounds which were not investigated in all assays (levocetirizine, mirtazapine, clozapine, doxepine), are given in the footnote to Table 2. For most of the hH_1R antagonists under study, the pK_b values were in the same range as the functional data

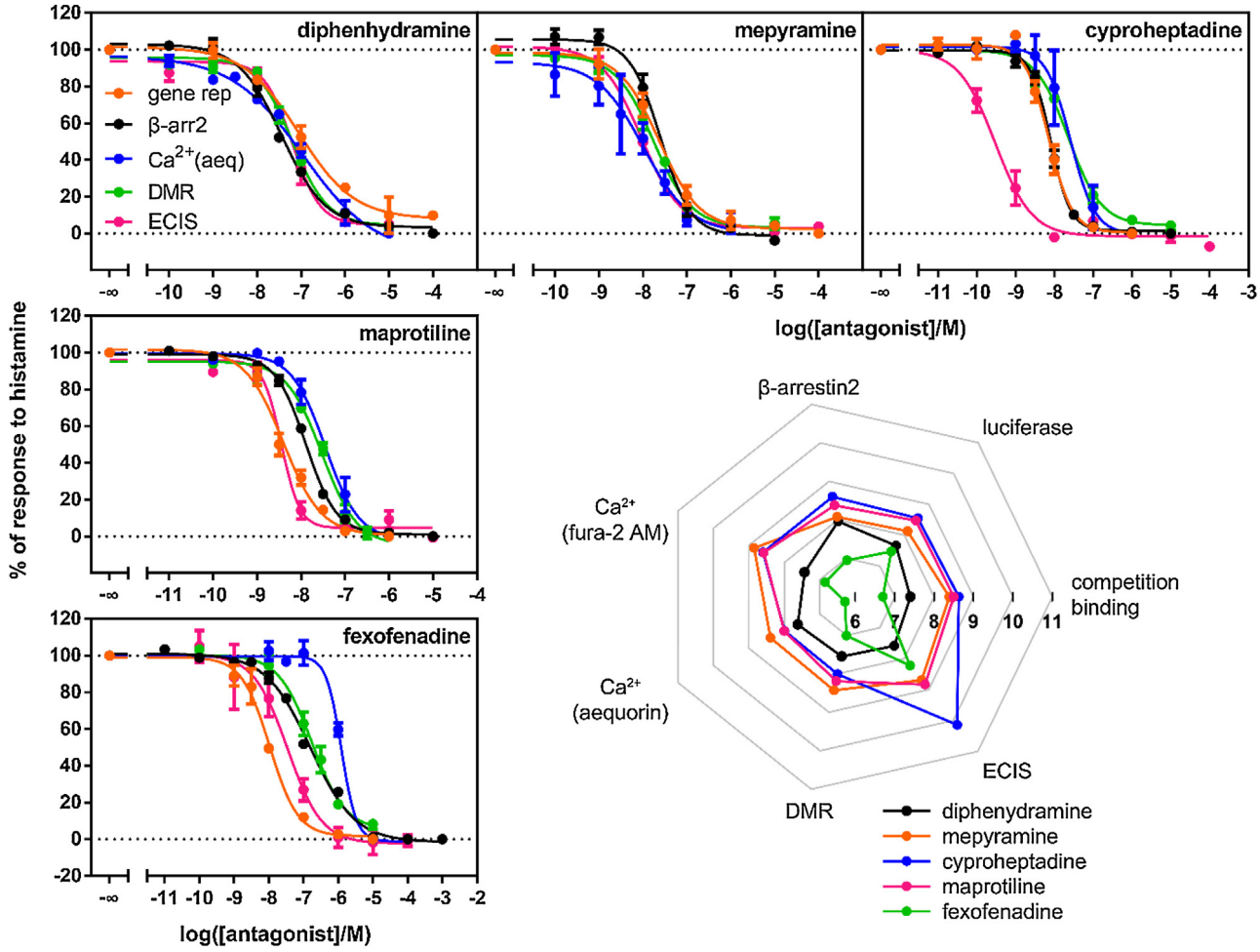

Fig. 6. Histamine H_1R antagonism of diphenhydramine, mepyramine, cyproheptadine, maprotiline and fexofenadine in five different assays. Inhibition curves and spider plot. Experiments were performed using genetically engineered HEK293T cells expressing the hH_1R and additional constructs; gene rep (luciferase gene reporter assay): HEK293T-CRE-Luc-hH1R cells; βarr2: (β-arrestin2 recruitment assay): HEK293T-ARRB2-H_1R cells; Ca^{2+}(aeq) (aequorin calcium assay): HEK293T-CRE-Luc-hH_1R-mtAEQ cells; DMR and ECIS (impedimetry): HEK293T-CRE-Luc-hH_1R-hMSR1 cells. Histamine was used at a concentration producing approximately 80% of the maximal response in the respective assay. Data were normalized to a solvent control and the EC_{80}-activation of histamine in each system. Data represent means ± SEM from at least three independent experiments performed in triplicate.

(GTPase assay, Sf9 cell membranes) from the literature [74,78] and the binding data from our laboratory (Table 2). However, there were some discrepancies, as becomes obvious from the inhibition curves and the spider plot in Fig. 6, in particular, in case of fexofenadine, when studied in the aequorin assay, and for cyproheptadine in the impedimetric assay. The data gained from the impedimetric assay suggested 10- to 30-fold higher apparent affinity compared to the values determined by radioligand competition binding. Except for impedimetric readouts, experiments in the antagonist mode do not display a similarly strong assay-dependence for a given antagonist as observed in case of agonists (cf. spider plot in Fig. 6). However, there is a trend towards higher pK_b values in ECIS.

4. Conclusion

Label-free methods (DMR and ECIS) and various signaling pathway specific readouts were used for the characterization of H_1R agonists and antagonists on genetically engineered HEK293T cells, i. e., cells of an identical genetic background. For antagonists, the results from DMR were essentially compatible with those from conventional readouts, whereas the impedance-based data were inconsistent in some cases. ECIS, especially when performed in the antagonist mode, turned out to be less reliable and more prone to errors than DMR. In this context, the influence of the test compounds on the conductivity of the cell membrane plays a critical role. Therefore, substance-specific receptor-independent effects might contribute to the impedance change. Most pronounced differences between the various assays became obvious for agonists regarding both, potencies and efficacies, depending on the chemical structure of the ligand and the type of readout, reflecting the complexity of the assays performed in the agonist mode. These differences can only be explained in part. DMR appears to integrate both, G_q and G_i mediated signaling (Fig. 7), the main two pathways described for the H_1R, as does the gene reporter assay. By contrast, ECIS and calcium assays apparently only reflect G_q signaling. DMR, ECIS and the Fura-2 assays allow the investigation of cellular effects in real time, whereas gene reporter, aequorin, β-arrestin recruitment, GTPase and GTPγS assays are endpoint measurements. Distinct histamine H_1R ligands did not effect the different functional readouts in a uniform way, a phenomenon, which may indicate “functional selectivity” or “biased signaling”, provided that off-targets are not involved. As the latter cannot be excluded, in addition to different readouts, selective receptor agonists and antagonists as well as specific inhibitors of signaling pathways are required as pharmacological tools to reduce the risk of misinterpretation and pitfalls. In so far, label-free holistic

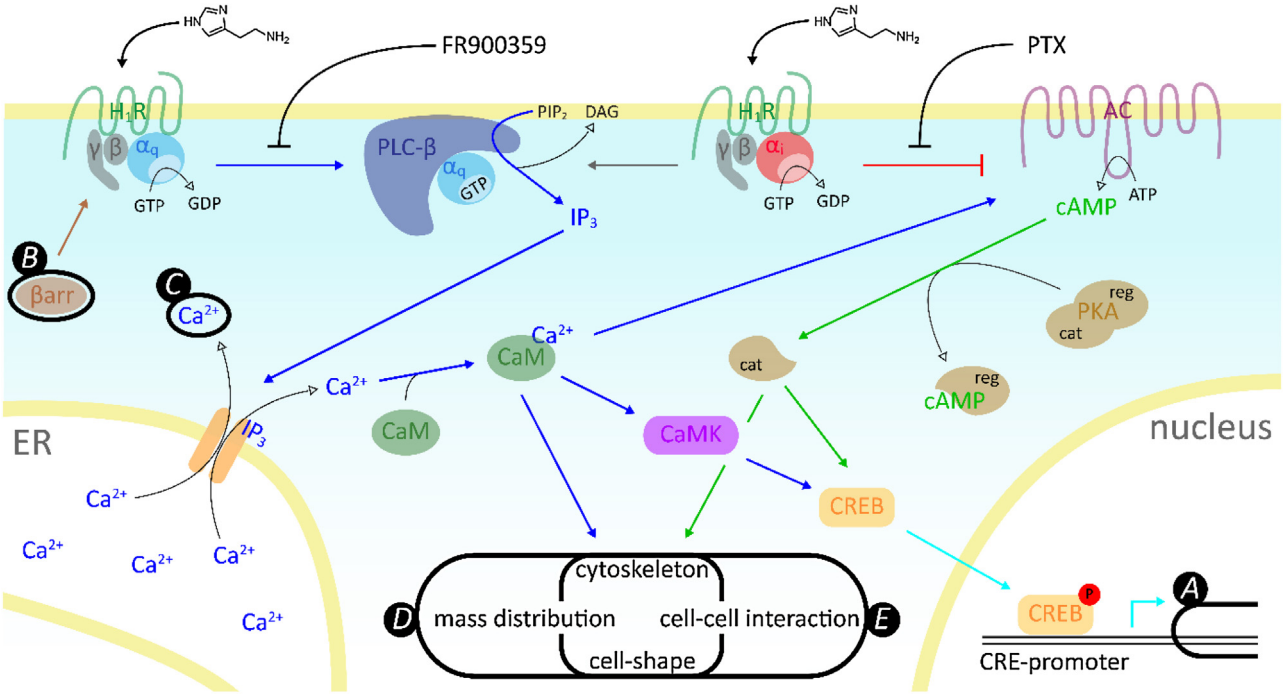

Assay		Readout	Modulation of the histamine signal by		Contribution to the readout
			FR900359 (1 µM)	PTX (100 ng/mL)	
A	gene reporter	luciferase activity	- 50%	+ 75%	G_q, G_i, (G_s ?)
B	β-arrestin recruitment	split luciferase complementation	n. d.	n. d.	β-arrestin1 or β-arrestin2
C	calcium mobilization (e.g. aequorin)	$[Ca^{2+}]_i$	- 100%	0%	G_q
D	DMR	wavelength shift	- 85%	- 100%	G_q, G_i
E	ECIS	impedance change	- 100%	- 10%	G_q, (G_i)

Fig. 7. Signaling pathways contributing to the H_1R mediated response in different assays.

methods such as DMR and ECIS are reminiscent of investigations on isolated organs and may be considered as "integrative pharmacology" at the cellular level. The question arises whether human cells constitutively expressing the receptor of interest and originating from the organ to be targeted should serve as more appropriate models than genetically engineered cells.

Conflict of interest

The authors declare that there are no conflicts of interest.

Acknowledgements

The authors are grateful to Elvira Schreiber, Maria Beer-Krön, Angelina Welsch, Christiane Luther, Esther Mönkemöller, Isabelle Nagmar and Lisa Forster for expert technical help and to Dr. Dorothée Möller (Friedrich-Alexander Universität, Erlangen-Nürnberg) for kindly providing D_2 receptor expressing HT-22 cells. A PhD student scholarship awarded to S.L. by the Hanns-Seidel-Stiftung and a PhD position awarded to T.L. from the International Doctoral Program "Receptor Dynamics" Elite Network of Bavaria are gratefully acknowledged. This study was supported by the Graduate Training Program GRK 1910 ("Medicinal Chemistry of Selective GPCR Ligands") of the Deutsche Forschungsgemeinschaft.

Appendix A. Supplementary data

Supplementary data associated with this article can be found, in the online version, at http://dx.doi.org/10.1016/j.phrs.2016.10.010.

References

[1] A.S. Ash, H.O. Schild, Receptors mediating some actions of histamine, Br. J. Pharmacol. Chemother. 27 (1966) 427–439.
[2] M.K. Church, M. Maurer, Antihistamines, Chem. Immunol. Allergy 100 (2014) 302–310.
[3] M.B. Emanuel, Histamine and the antiallergic antihistamines: a history of their discoveries, Clin. Exp. Allergy 29 (Suppl. 3) (1999) 1–11.
[4] P. Panula, P.L. Chazot, M. Cowart, R. Gutzmer, R. Leurs, W.L. Liu, H. Stark, R.L. Thurmond, H.L. Haas, International union of basic and clinical pharmacology. XCVIII. histamine receptors, Pharmacol. Rev. 67 (2015) 601–655.
[5] T. Kenakin, C. Watson, V. Muniz-Medina, A. Christopoulos, S. Novick, A simple method for quantifying functional selectivity and agonist bias, ACS Chem. Neurosci. 3 (2012) 193–203.
[6] A.M. Ferrie, V. Goral, C. Wang, Y. Fang, Label-free functional selectivity assays, Methods Mol. Biol. 1272 (2015) 227–246.

[7] T. Kenakin, Functional selectivity and biased receptor signaling, J. Pharmacol. Exp. Ther. 336 (2011) 296–302.
[8] T. Kenakin, L.J. Miller, Seven transmembrane receptors as shapeshifting proteins: the impact of allosteric modulation and functional selectivity on new drug discovery, Pharmacol. Rev. 62 (2010) 265–304.
[9] M. Marti-Solano, F. Sanz, M. Pastor, J. Selent, A dynamic view of molecular switch behavior at serotonin receptors: implications for functional selectivity, PLoS One 9 (2014) e109312.
[10] R. Seifert, Functional selectivity of G-protein-coupled receptors: from recombinant systems to native human cells, Biochem. Pharmacol. 86 (2013) 853–861.
[11] W. Stallaert, A. Christopoulos, M. Bouvier, Ligand functional selectivity and quantitative pharmacology at G protein-coupled receptors, Expert Opin. Drug Discov. 6 (2011) 811–825.
[12] L. Zhou, L.M. Bohn, Functional selectivity of GPCR signaling in animals, Curr. Opin. Cell Biol. 27 (2014) 102–108.
[13] T. Aristotelous, A.L. Hopkins, I. Navratilova, Surface plasmon resonance analysis of seven-transmembrane receptors, Methods Enzymol. 556 (2015) 499–525.
[14] H. Deng, H. Sun, Y. Fang, Label-free cell phenotypic assessment of the biased agonism and efficacy of agonists at the endogenous muscarinic M3 receptors, J. Pharmacol. Toxicol. Methods 68 (2013) 323–333.
[15] Y. Fang, A.M. Ferrie, E. Tran, Resonant waveguide grating biosensor for whole-cell GPCR assays, Methods Mol. Biol. 552 (2009) 239–252.
[16] Y. Fang, A.G. Frutos, R. Verklereen, Label-free cell-based assays for GPCR screening, Comb. Chem. High Throughput Screen. 11 (2008) 357–369.
[17] M. Grundmann, E. Kostenis, Label-free biosensor assays in GPCR screening, Methods Mol. Biol. 1272 (2015) 199–213.
[18] R.P. McGuinness, J.M. Proctor, D.L. Gallant, C.J. van Staden, J.T. Ly, F.L. Tang, P.H. Lee, Enhanced selectivity screening of GPCR ligands using a label-free cell based assay technology, Comb. Chem. High Throughput Screen. 12 (2009) 812–823.
[19] K. Miyano, Y. Sudo, A. Yokoyama, K. Hisaoka-Nakashima, N. Morioka, M. Takebayashi, Y. Nakata, Y. Higami, Y. Uezono, History of the G protein-coupled receptor (GPCR) assays from traditional to a state-of-the-art biosensor assay, J. Pharmacol. Sci. 126 (2014) 302–309.
[20] S. Lieb, S. Michaelis, N. Plank, G. Bernhardt, A. Buschauer, J. Wegener, Label-free analysis of GPCR-stimulation: the critical impact of cell adhesion, Pharmacol. Res. 108 (2016) 65–74.
[21] Y. Fang, Label-free biosensors for cell biology, Int. J. Electrochem. (2011), Article ID 460850.
[22] N. Yu, J.M. Atienza, J. Bernard, S. Blanc, J. Zhu, X. Wang, X. Xu, Y.A. Abassi, Real-time monitoring of morphological changes in living cells by electronic cell sensor arrays: an approach to study G protein-coupled receptors, Anal. Chem. 78 (2006) 35–43.
[23] R. Halai, D.E. Croker, J.Y. Suen, D.P. Fairlie, M.A. Cooper, A comparative study of impedance versus optical label-free systems relative to labelled assays in a predominantly Gi coupled GPCR (C5aR) signalling, Biosensors (Basel) 2 (2012) 273–290.
[24] N. Ke, K. Nguyen, J. Irelan, Y.A. Abassi, Multidimensional GPCR profiling and screening using impedance-based label-free and real-time assay, Methods Mol. Biol. 1272 (2015) 215–226.
[25] M.F. Peters, F. Vaillancourt, M. Heroux, M. Valiquette, C.W. Scott, Comparing label-free biosensors for pharmacological screening with cell-based functional assays, Assay Drug Dev. Technol. 8 (2010) 219–227.
[26] R. Schröder, N. Janssen, J. Schmidt, A. Kebig, N. Merten, S. Hennen, A. Muller, S. Blattermann, M. Mohr-Andra, S. Zahn, J. Wenzel, N.J. Smith, J. Gomeza, C. Drewke, G. Milligan, K. Mohr, E. Kostenis, Deconvolution of complex G protein-coupled receptor signaling in live cells using dynamic mass redistribution measurements, Nat. Biotechnol. 28 (2010) 943–949.
[27] M.J. Adjobo-Hermans, J. Goedhart, L. van Weeren, S. Nijmeijer, E.M. Manders, S. Offermanns, T.W. Gadella Jr., Real-time visualization of heterotrimeric G protein Gq activation in living cells, BMC Biol. 9 (2011) 32.
[28] S. Gutowski, A. Smrcka, L. Nowak, D.G. Wu, M. Simon, P.C. Sternweis, Antibodies to the alpha q subfamily of guanine nucleotide-binding regulatory protein alpha subunits attenuate activation of phosphatidylinositol 4,5-bisphosphate hydrolysis by hormones, J. Biol. Chem. 266 (1991) 20519–20524.
[29] J. Lu, J. Li, Label-free imaging of dynamic and transient calcium signaling in single cells, Angew. Chem. Int. Ed. 54 (2015) 13576–13580.
[30] E. Verdonk, K. Johnson, R. McGuinness, G. Leung, Y.-W. Chen, H.R. Tang, J.M. Michelotti, V.F. Liu, Cellular dielectric spectroscopy: a label-free comprehensive platform for functional evaluation of endogenous receptors, Assay Drug Dev. Technol. 4 (2006) 609–619.
[31] R. Seifert, L. Grünbaum, G. Schultz, Histamine H1-receptors in HL-60 monocytes are coupled to Gi-proteins and pertussis toxin-insensitive G-proteins and mediate activation of Ca2+ influx without concomitant Ca2+ mobilization from intracellular stores, Naunyn-Schmiedeberg's Arch. Pharmacol. 349 (1994) 355–361.
[32] Y.X. Wang, M.I. Kotlikoff, Signalling pathway for histamine activation of non-selective cation channels in equine tracheal myocytes, J. Physiol. 523 (Pt. 1) (2000) 131–138.
[33] A.J. Robinson, J.M. Dickenson, Activation of the p38 and p42/p44 mitogen-activated protein kinase families by the histamine H(1) receptor in DDT(1)MF-2 cells, Br. J. Pharmacol. 133 (2001) 1378–1386.
[34] T.A. Esbenshade, C.H. Kang, K.M. Krueger, T.R. Miller, D.G. Witte, J.M. Roch, J.N. Masters, A.A. Hancock, Differential activation of dual signaling responses by human H1 and H2 histamine receptors, J. Recept. Signal Transduct. 23 (2003) 17–31.
[35] R.A. Bakker, S.B. Schoonus, M.J. Smit, H. Timmerman, R. Leurs, Histamine H(1)-receptor activation of nuclear factor-kappa B: roles for G beta gamma- and G alpha(q/11)-subunits in constitutive and agonist-mediated signaling, Mol. Pharmacol. 60 (2001) 1133–1142.
[36] P.J. Brighton, S. Rana, R.J. Challiss, J.C. Konje, J.M. Willets, Arrestins differentially regulate histamine- and oxytocin-evoked phospholipase C and mitogen-activated protein kinase signalling in myometrial cells, Br. J. Pharmacol. 162 (2011) 1603–1617.
[37] J.M. Willets, A.H. Taylor, H. Shaw, J.C. Konje, R.A. Challiss, Selective regulation of H1 histamine receptor signaling by G protein-coupled receptor kinase 2 in uterine smooth muscle cells, Mol. Endocrinol. 22 (2008) 1893–1907.
[38] E. Khoury, L. Nikolajev, M. Simaan, Y. Namkung, S.A. Laporte, Differential regulation of endosomal GPCR/beta-arrestin complexes and trafficking by MAPK, J. Biol. Chem. 289 (2014) 23302–23317.
[39] J.S. Paradis, S. Ly, E. Blondel-Tepaz, J.A. Galan, A. Beautrait, M.G. Scott, H. Enslen, S. Marullo, P.P. Roux, M. Bouvier, Receptor sequestration in response to beta-arrestin-2 phosphorylation by ERK1/2 governs steady-state levels of GPCR cell-surface expression, Proc. Natl. Acad. Sci. U. S. A. 112 (2015) E5160–5168.
[40] A. Strasser, H.-J. Wittmann, M. Kunze, S. Elz, R. Seifert, Molecular basis for the selective interaction of synthetic agonists with the human histamine H1-receptor compared with the guinea pig H1-receptor, Mol. Pharmacol. 75 (2009) 454–465.
[41] C. Leschke, S. Elz, M. Garbarg, W. Schunack, Synthesis and histamine H1 receptor agonist activity of a series of 2-phenylhistamines 2-heteroarylhistamines, and analogues, J. Med. Chem. 38 (1995) 1287–1294.
[42] V. Zingel, C. Leschke, W. Schunack, Developments in histamine H1-receptor agonists, Prog. Drug Res. 44 (1995) 49–85.
[43] S. Elz, K. Kramer, H.H. Pertz, H. Detert, A.M. ter Laak, R. Kuhne, W. Schunack, Histaprodifens: synthesis, pharmacological in vitro evaluation, and molecular modeling of a new class of highly active and selective histamine H(1)-receptor agonists, J. Med. Chem. 43 (2000) 1071–1084.
[44] B. Striegl, Synthese und funktionelle in-vitro-Pharmakologie neuer Histamin-H1-Rezeptoragonisten aus der Suprahistaprodifen-Reihe, Dissertation, Universität Regensburg, 2007 http://epub.uni-regensburg.de/10494/.
[45] U. Nordemann, D. Wifling, D. Schnell, G. Bernhardt, H. Stark, R. Seifert, A. Buschauer, Luciferase reporter gene assay on human, murine and rat histamine H_4 receptor orthologs: correlations and discrepancies between distal and proximal readouts, PLoS One 8 (2013) e73961.
[46] A. Matsumoto, M. Naito, H. Itakura, S. Ikemoto, H. Asaoka, I. Hayakawa, H. Kanamori, H. Aburatani, F. Takaku, H. Suzuki, Human macrophage scavenger receptors: primary structure, expression, and localization in atherosclerotic lesions, Proc. Natl. Acad. Sci. U. S. A. 87 (1990) 9133–9137.
[47] N. Misawa, A.K. Kafi, M. Hattori, K. Miura, K. Masuda, T. Ozawa, Rapid and high-sensitivity cell-based assays of protein–protein interactions using split click beetle luciferase complementation: an approach to the study of G-protein-coupled receptors, Anal. Chem. 82 (2010) 2552–2560.
[48] R. Ziemek, E. Schneider, A. Kraus, C. Cabrele, A.G. Beck-Sickinger, G. Bernhardt, A. Buschauer, Determination of affinity and activity of ligands at the human neuropeptide Y Y4 receptor by flow cytometry and aequorin luminescence, J. Recept. Signal Transduct. 27 (2007) 217–233.
[49] M. Müller, S. Knieps, K. Gessele, S. Dove, G. Bernhardt, A. Buschauer, Synthesis and neuropeptide Y Y1 receptor antagonistic activity of N,N-disubstituted omega-guanidino- and omega-aminoalkanoic acid amides, Arch. Pharm. (Weinheim) 330 (1997) 333–342.
[50] J. Mosandl, Radiochemical and Luminescence-based Binding and Functional Assays for Human Histamine Receptors Using Genetically Engineered Cells. Doctoral Thesis, University of Regensburg, 2009.
[51] A. Gupta, M. Gillard, B. Christophe, P. Chatelain, R. Massingham, M. Hammarlund-Udenaes, Peripheral and central H1 histamine receptor occupancy by levocetirizine, a non-sedating antihistamine; a time course study in the guinea pig, Br. J. Pharmacol. 151 (2007) 1129–1136.
[52] Y. Cheng, W.H. Prusoff, Relationship between the inhibition constant (K_I) and the concentration of inhibitor which causes 50 per cent inhibition (I_{50}) of an enzymatic reaction, Biochem. Pharmacol. 22 (1973) 3099–3108.
[53] R. Schröder, J. Schmidt, S. Blattermann, L. Peters, N. Janssen, M. Grundmann, W. Seemann, D. Kaufel, N. Merten, C. Drewke, J. Gomeza, G. Milligan, K. Mohr, E. Kostenis, Applying label-free dynamic mass redistribution technology to frame signaling of G protein-coupled receptors noninvasively in living cells, Nat. Protoc. 6 (2011) 1748–1760.
[54] J. Stolwijk, K. Matrougui, C. Renken, M. Trebak, Impedance analysis of GPCR-mediated changes in endothelial barrier function: overview and fundamental considerations for stable and reproducible measurements, Pflügers Arch. – Eur. J. Physiol. 467 (2015) 2193–2218.
[55] M. Cotton, A. Claing, G protein-coupled receptors stimulation and the control of cell migration, Cell. Signal. 21 (2009) 1045–1053.
[56] A.K. Robbins, R.A. Horlick, Macrophage scavenger receptor confers an adherent phenotype to cells in culture, BioTechniques 25 (1998) 240–244.
[57] M. Fujioka, S. Koda, Y. Morimoto, K. Biemann, Structure of Fr900359, a cyclic depsipeptide from *Ardisia crenata* Sims, J. Org. Chem. 53 (1988) 2820–2825.

[58] R. Schrage, A.-L. Schmitz, E. Gaffal, S. Annala, S. Kehraus, D. Wenzel, K.M. Büllesbach, T. Bald, A. Inoue, Y. Shinjo, S. Galandrin, N. Shridhar, M. Hesse, M. Grundmann, N. Merten, T.H. Charpentier, M. Martz, A.J. Butcher, T. Slodczyk, S. Armando, M. Effern, Y. Namkung, L. Jenkins, V. Horn, A. Stößel, H. Dargatz, D. Tietze, D. Imhof, C. Galés, C. Drewke, C.E. Müller, M. Hölzel, G. Milligan, A.B. Tobin, J. Gomeza, H.G. Dohlman, J. Sondek, T.K. Harden, M. Bouvier, S.A. Laporte, J. Aoki, B.K. Fleischmann, K. Mohr, G.M. König, T. Tüting, E. Kostenis, The experimental power of FR900359 to study Gq-regulated biological processes, Nat. Commun. 6 (2015) 10156.
[59] R. Seifert, A. Hoer, S. Offermanns, A. Buschauer, W. Schunack, Histamine increases cytosolic Ca2+ in dibutyryl-cAMP-differentiated HL-60 cells via H1 receptors and is an incomplete secretagogue, Mol. Pharmacol. 42 (1992) 227–234.
[60] H. Enslen, P. Sun, D. Brickey, S.H. Soderling, E. Klamo, T.R. Soderling, Characterization of Ca2+/calmodulin-dependent protein kinase IV. Role in transcriptional regulation, J. Biol. Chem. 269 (1994) 15520–15527.
[61] G.E. Hardingham, F.H. Cruzalegui, S. Chawla, H. Bading, Mechanisms controlling gene expression by nuclear calcium signals, Cell. Calcium 23 (1998) 131–134.
[62] H. Ma, R.D. Groth, S.M. Cohen, J.F. Emery, B. Li, E. Hoedt, G. Zhang, T.A. Neubert, R.W. Tsien, gammaCaMKII shuttles Ca(2)(+)/CaM to the nucleus to trigger CREB phosphorylation and gene expression, Cell 159 (2014) 281–294.
[63] G.D. Ferguson, D.R. Storm, Why salcium-stimulated adenylyl cyclases? Physiology 19 (2004) 271–276.
[64] B.T. Gjertsen, G. Mellgren, A. Otten, E. Maronde, H.G. Genieser, B. Jastorff, O.K. Vintermyr, G.S. McKnight, S.O. Doskeland, Novel (Rp)-cAMPS analogs as tools for inhibition of cAMP-kinase in cell culture. Basal cAMP-kinase activity modulates interleukin-1 beta action, J. Biol. Chem. 270 (1995) 20599–20607.
[65] A.D. Federman, B.R. Conklin, K.A. Schrader, R.R. Reed, H.R. Bourne, Hormonal stimulation of adenylyl cyclase through Gi-protein beta gamma subunits, Nature 356 (1992) 159–161.
[66] T.M. Cabrera-Vera, J. Vanhauwe, T.O. Thomas, M. Medkova, A. Preininger, M.R. Mazzoni, H.E. Hamm, Insights into G protein structure function, and regulation, Endocr. Rev. 24 (2003) 765–781.
[67] S. Müller, M.J. Lohse, The role of G-protein beta gamma subunits in signal transduction, Biochem. Soc. Trans. 23 (1995) 141–148.
[68] N. Wettschureck, S. Offermanns, Mammalian G proteins and their cell type specific functions, Physiol. Rev. 85 (2005) 1159–1204.
[69] Z.-G. Gao, K.A. Jacobson, On the selectivity of the Gαq inhibitor UBO-QIC: a comparison with the Gαi inhibitor pertussis toxin, Biochem. Pharmacol. 107 (2016) 59–66.
[70] D.M. Lehmann, A.M. Seneviratne, A.V. Smrcka, Small molecule disruption of G protein beta gamma subunit signaling inhibits neutrophil chemotaxis and inflammation, Mol. Pharmacol. 73 (2008) 410–418.
[71] T.M. Bonacci, J.L. Mathews, C. Yuan, D.M. Lehmann, S. Malik, D. Wu, J.L. Font, J.M. Bidlack, A.V. Smrcka, Differential targeting of Gbetagamma-subunit signaling with small molecules, Science 312 (2006) 443–446.
[72] K.A. Neve, J.K. Seamans, H. Trantham-Davidson, Dopamine receptor signaling, J. Recept. Signal Transduct. 24 (2004) 165–205.
[73] A. Strasser, B. Striegl, H.J. Wittmann, R. Seifert, Pharmacological profile of histaprodifens at four recombinant histamine H1 receptor species isoforms, J. Pharmacol. Exp. Ther. 324 (2008) 60–71.
[74] R. Seifert, K. Wenzel-Seifert, T. Bürckstümmer, H.H. Pertz, W. Schunack, S. Dove, A. Buschauer, S. Elz, Multiple differences in agonist and antagonist pharmacology between human and Guinea pig histamine H1-receptor, J. Pharmacol. Exp. Ther. 305 (2003) 1104–1115.
[75] R.H. Oakley, S.A. Laporte, J.A. Holt, M.G. Caron, L.S. Barak, Differential affinities of visual arrestin beta arrestin1, and beta arrestin2 for G protein-coupled receptors delineate two major classes of receptors, J. Biol. Chem. 275 (2000) 17201–17210.
[76] R. Schrage, A. De Min, K. Hochheiser, E. Kostenis, K. Mohr, Superagonism at G protein-coupled receptors and beyond, Br. J. Pharmacol. (2015), http://dx.doi.org/10.1111/bph.13278.
[77] S. Wilson, J.K. Chambers, J.E. Park, A. Ladurner, D.W. Cronk, C.G. Chapman, H. Kallender, M.J. Browne, G.J. Murphy, P.W. Young, Agonist potency at the cloned human beta-3 adrenoceptor depends on receptor expression level and nature of assay, J. Pharmacol. Exp. Ther. 279 (1996) 214–221.
[78] H. Appl, T. Holzammer, S. Dove, E. Haen, A. Strasser, R. Seifert, Interactions of recombinant human histamine H(1)R, H(2)R H(3)R, and H(4)R receptors with 34 antidepressants and antipsychotics, Naunyn-Schmiedeberg's Arch. Pharmacol. 385 (2012) 145–170.